Environmental Pollution 261 (2020) 114186

Contents lists available at ScienceDirect

Environmental Pollution

journal homepage: www.elsevier.com/locate/envpol

Effect of northern boreal forest fires on PAH fluctuations across the arctic☆

Jinmu Luo [a], Yunman Han [a], Yuan Zhao [a], Yufei Huang [a], Xinrui Liu [a], Shu Tao [a], Junfeng Liu [a], Tao Huang [b], Linfei Wang [a], Kaijie Chen [a], Jianmin Ma [a, *]

[a] Laboratory for Earth Surface Processes, College of Urban and Environmental Sciences, Peking University, Beijing, 100871, China
[b] Key Laboratory for Environmental Pollution Prediction and Control, Gansu Province, College of Earth and Environmental Sciences, Lanzhou University, Lanzhou, 730000, PR China

ARTICLE INFO

Article history:
Received 18 October 2019
Received in revised form
11 February 2020
Accepted 13 February 2020
Available online 17 February 2020

Keywords:
Polycyclic aromatic hydrocarbons
BaP
Biomass burning
Emission
Source apportionment

ABSTRACT

Polycyclic aromatic hydrocarbons (PAHs) are formed by the incomplete combustion of fossil fuels and forest or biomass burning. PAHs undergo long-range atmospheric transport, as evidenced by in situ observations across the Arctic. However, monitored atmospheric concentrations of PAHs indicate that ambient PAH levels in the Arctic do not follow the declining trend of worldwide anthropogenic PAH emissions since the 2000s, suggesting missing sources of PAHs in the Arctic or other places across the Northern Hemisphere. To trace origins and causes for the increasing trend of PAHs in the Arctic, the present study reconstructed PAH emissions from forest fires in the northern boreal forest derived by combining forest carbon stocks and MODIS burned area. We examined the statistical relationships of forest biomass, MODIS burned area, emission factors, and combustion efficiency with different PAH congeners. These relationships were then employed to construct PAH emission inventories from forest biomass burning. We show that for some PAH congeners, for example, benzo[a]pyrene (BaP)—the forest-fire-induced air emissions are almost one order of magnitude higher than previous emission inventories in the Arctic. A global-scale atmospheric chemistry model, GEOS-Chem, was used to simulate air concentrations of BaP, a representative PAH congener primarily emitted from biomass burning, and to quantify the response of BaP to wildfires in the northern boreal forest. The results showed that BaP emissions from wildfires across the northern boreal forest region played a significant role in the contamination and interannual fluctuations of BaP in Arctic air. A source-tagging technique was applied in tracking the origins of BaP pollution from different northern boreal forest regions. We also show that the response of BaP pollution at different Arctic monitoring sites depends on the intensity of human activities.

1. Introduction

Unprecedented wildfires in the Arctic in the spring and early summer of 2019, attributable to record high air temperatures and declining precipitation, have raised considerable concerns about the release of more carbon dioxide and harmful air pollutants into the Arctic atmosphere (WMO, 2019). Wildfires are considered to be a major source of air pollutants in the Arctic (Stohl et al., 2007; Treffeisen et al., 2007). Among those harmful chemicals released from wildfires, polycyclic aromatic hydrocarbons (PAHs) should receive special attention because PAHs are a class of byproducts from incomplete anthropogenic and natural organic material combustion. PAHs are toxic, carcinogenic, mutagenic, and teratogenic, and cause risks to human health. Due to their physicochemical properties, PAHs can undergo long-range transport and are widespread in the ambient air (Friedman and Selin, 2016; Ravindra et al., 2008; Wilcke, 2007). The long-range atmospheric transport of PAHs has been particularly evidenced by their presence in the pristine Arctic environment (Hung et al., 2005; Laender et al., 2011; Friedman and Selin, 2012; Yu et al., 2019). Following worldwide bans and restrictions on the use of many persistent organic pollutants (POPs), including PAHs (the United Nations Economic Commission for Europe (UNECE) Convention on Long-range

☆ This paper has been recommended for acceptance by Dr. Admir Créso Targino.
* Corresponding author.
E-mail address: jmma@pku.edu.cn (J. Ma).

https://doi.org/10.1016/j.envpol.2020.114186
0269-7491/

Transboundary Air Pollution), from the late 1970s, their levels in the ambient air have been declining worldwide (Kong et al., 2014; Ma et al., 2016, 2011). However, during the 2000s, the declining trend of many POPs and PAHs has slowed down, and concentrations of some of these chemicals showed an intermittent increase (Hung et al., 2016; Ma et al., 2016). A recent investigation (Yu et al., 2019) reported inclines of three PAH congeners—PHE (phenanthrene), BaP, and PYR (pyrene)—in Arctic air in the mid-2000s and early 2010s, opposite to the declining trend of worldwide anthropogenic PAH emissions. Such increasing trends were partly attributed to forest fires and Arctic warming. Rising temperature could enhance the partitioning of organic chemicals from liquid and solid phase to gas phase, leading to their secondary emission from water and soil into the air, increased ice melt, and more open oceans in the Arctic, providing another means for historically archived contaminants in the arctic environment to be released into the atmosphere (Ma et al., 2011, 2016).

Forest fires have also been connected to climate warming in the 21st century, particularly in the past two decades, which is evidenced by the considerably increasing incidence and frequency of forest fires (Gillett et al., 2004; Malevsky-Malevich et al., 2008; Stocks et al., 1998; Kim et al., 2020). Yu et al. (2019) assessed the potential associations between remotely-sensed forest fire data and PAH fluctuation in the Arctic and linked increasing PAH concentrations observed in the Arctic with wildfires that are themselves associated with increasing temperature trends. On the other hand, Friedman et al. (2014) showed that the effect of climate warming on PAH transport into and out of the Arctic via the atmosphere is insignificant, and other studies have also indicated that rising temperature plays a moderate role in the long-term trends of POPs in the Arctic (Kong et al., 2014; Ma et al., 2016). While climate change and forest fires are thought to be important factors influencing POPs, such influence has not been sufficiently quantified and identified from worldwide PAH sources. Previous studies have shown that PAH emissions from wildfires and deforestation could contribute considerably to their global total levels (Shen et al., 2013; Zhang and Tao, 2009; Galarneau et al., 2007; Schifman and Boving., 2015; Muntean et al., 2016; Miura et al., 2019; Zhao et al., 2019). More importantly, located in 40°N–85°N, the northern boreal forest has a biomass storage of over 53.9 PgC, accounting for 13.701% of the total biomass in the world (Pan et al., 2013). As byproducts of incomplete combustion of northern boreal wood burning, PAHs, black carbon, and other aerosols could more readily reach the polar environment because of the proximity of the northern boreal forest to the Arctic; this implies that the Arctic environment is likely to be more sensitive to biomass burning than many parts of the world.

The lack of accurately accounted wildfire-induced emissions in the current PAH emission inventories has resulted in large uncertainties in the prediction of the PAH environmental fate and fluctuations across the Arctic (Friedman et al., 2012; 2014; Yu et al., 2019). To fill knowledge gaps, the present study aims to (1) develop an updated PAH emission inventory which could significantly improve the PAH release from forest fire biomass burning—using, for the first time ever, the carbon stock data; (2) predict changes in PAH concentrations in the Arctic since 2000, and validate the modeled data with routinely measured data at three Arctic sites using an innovated atmospheric chemistry model; and (3) quantify the contribution of the PAH emissions from northern boreal forest fires to their fluctuations in the polar regions. In a recent source apportionment analysis for PAHs in the Arctic, Yu et al. found that biomass burning dominated fluctuation of 5–6 ring PAHs, including BaP, in the Arctic after 2004, whereas coal combustion and air-surface exchange (secondary emission) contributed primarily to 2–3 ring PAH levels, such as PHE (2019). As biomass burning favors the formation of particle-phase PAHs, the present study selected BaP, a particle-bound PAH congener, as a representative PAH congener in our atmospheric chemistry modeling using GEOS-Chem by implementing the new BaP emission inventory from forest fire biomass burning. The results were further used to justify the significance of forest fires in the temporal trends and spatial distributions of PAHs in the Arctic.

2. Materials and methods

2.1. Global forest carbon stocks

As a dominant terrestrial ecosystem on the earth, forest biomass (carbon stocks, PgC) covers over 81% of the total biomass in the world and plays an important role in the earth's climate system (Bar-On et al., 2018; Pan et al., 2013). The distribution and pattern of global forest carbon stocks remain poorly quantified, and in particular, a finer resolution carbon stock map is still lacking. Traditionally, there are two ways to obtain global forest carbon stock maps. The first method is referred to as the up-down approach, which is also known as remote sensing. Many previous studies have used space-on satellite instruments to successfully detect plant carbon stocks on the Earth's surface (Dong et al., 2003; Saatchi et al., 2011; Thurner et al., 2014; Zhang and Kondragunta, 2006). In situ measurement validation results show that satellite remote sensing is a very useful technique to estimate and monitor forest carbon stocks on a large scale. However, different satellite instruments (e.g., OPTICAL, SARS, and LIDAR) often yield different results. The second approach is the bottom-up approach, in which the forest inventory is compiled through long-term measurements and field investigations. In most cases, these two approaches are combined to compile a global forest carbon stock inventory.

In the present study, we collected two widely used bottom-up forest (carbon stock) inventories from Pan et al. (2011) and the Global Forest Resources Assessment (FRA 2015) . For convenience, we clustered the carbon stocks at a continent level to show the difference between the two inventories. Table 1 presents the carbon stocks from the two forest inventories. The most obvious differences between the two inventories are found in Africa and the Americas, while consistent in the rest of world. Baccini et al. (2012) indicated that (FRA 2010) might underestimate 20% of the vegetation carbon stocks in tropical regions. There were also other limitations in the FRA datasets, including incomplete country reporting, inaccurate reporting, the lack of measurement support in some countries, and insufficient information of specific forest type or subnational distribution of forest resources, as summarized by MacDicken (2015). For example, we noticed that FRA missed some

Table 1
Living biomass or carbon stocks (unit: PgC) in 2010 collected from FRA (2010) and Pan et al. (2011) in different continents, countries, and regions.

	Africa	Asia	Canada	Europe	China	Americas	Russia	USA	Oceania	Mid-East
FRA	62.75[a]	42.15	14.408	11.074	5.817	127.023[a]	32.157	15.711	9.403	0.888
Pan et al.	81.80	43.00	14.400	11.80	5.35	141.50	36.00	18.4	7.8	0[a]

[a] Missing data was reported in these continents and regions.

datasets in African and American countries. In these countries, we used the datasets from Pan et al. (2011) in place of the missing FRA data. The carbon stocks provided by Pan et al. (2011) were also subject to critical data gaps, particularly lacking boreal forest areas in North America. In these areas, we still used FRA carbon stock data. It should be recognized that these two datasets might not be completely consistent. Further uncertainty analysis of carbon stock data applied in PAH emission inventory will be presented in section 2.5 and the Supplementary. The continuous assessment in the FRA plan is for every five years, and the dataset is at the country level (the next forest resource assessment will be conducted in 2020). The final carbon stock map at the country level (Fig. S1) was created using the data from the FRA for all countries except for those in Africa, the Americas, and China, for which FRA did not provide sufficient carbon stock data. Given that the data from FRA and Pan et al. (2011) were available for every 5 years only, a linear regression model was established by assuming that forest growth, regrowth, and deforestation altered linearly to create annual carbon stocks in those years without measured data.

We used the spatial proxy data to downscale the country-level carbon stocks (Fig. S1) into a grid map (Erb et al., 2018). Among many tree properties, height (m) is a critical factor in estimates of forest carbon stocks (Erb et al., 2016; Fang et al., 2006) and is more easily accessed than other parameters. We chose the global canopy height (m, Fig. S2) provided by Simard et al. (2011) as a spatial proxy to downscale large-scale carbon stocks to the gridded map. The resulting map of carbon stocks has the same spatial resolution as the gridded tree height map at 0.05° × 0.05° latitude/longitude. It should be noted that we only collected the forest biomass from two forest inventories. In a realistic Earth surface terrestrial ecosystem, prairie, savanna, and grassland carbon stocks are also part of the global plant biomass, and biomass burning from these annual herbs is also significant (Haberl et al., 2007; Seiler and Crutzen, 1980; Vakkari et al., 2018). To take this part of biomass burning into account, we collected the annual amount of net primary production (NPP) from the Moderate Resolution Imaging Spectroradiometer (MODIS) satellite dataset MOD17A3H (https://lpdaac.usgs.gov/product_search/, last accessed on July 25, 2019) as the annual herb carbon stocks (Erb et al., 2016; Haberl et al., 2007). Yearly NPP data at a 500 m resolution from the MOD17A3H were also gridded into a resolution of 0.05° × 0.05° latitude/longitude. The resulting biomass was then added to the forest biomass directly. The gridded global forest carbon stocks in 2015 are shown in Fig. 1.

2.2. Emission factor and combustion efficiency

To quantify the PAH emission rate from forest fires or biomass burning, three key factors need to be taken into consideration: (1) how much of the surface biomass was burned; (2) the quantity of the burning carbon is transferred into the target pollutant; and (3) during the burning process, what is the combustion efficiency of the burning plants? The second and third factors can be defined as the emission factors and combustion efficiency, respectively. The emission factors for PAHs via biomass burning have been extensively investigated (Jenkins et al., 1996). The reported emission factors for 16 PAHs from previous studies vary from 5 to 683 mg/kg for dry matter and from 0.14 to 8.2 mg/kg for BaP for Europe confiner species, savanna grass, African hardwoods, and German and Indonesian peat. Field and lab studies were conducted to create PAH emission factors in cook stoves, fireplaces, and residential furnaces (Kakareka et al., 2005; Kim Oanh et al., 2005, 1999; Lee et al., 2005; Schauer et al., 2001). Table 2 shows the emission

Table 2
BaP emission factors collected from the literature.

Biomass type	Emission factor (mg/kg)	References
Pine with Greens	BaP 1	Iinuma et al. (2007)
Pine	BaP 0.35	Jenkins et al. (1996)
Fir	BaP 0.19	
Pine wood	BaP 0.38–1.59	Kim Oanh et al. (2005)
Wood fuel	BaP 0.693	Kim Oanh et al. (2005)
Pine	BaP 0.712	Schauer et al. (2001)
Oak	BaP 0.245	
Hard wood	BaP 0.14	Lee et al. (2005)

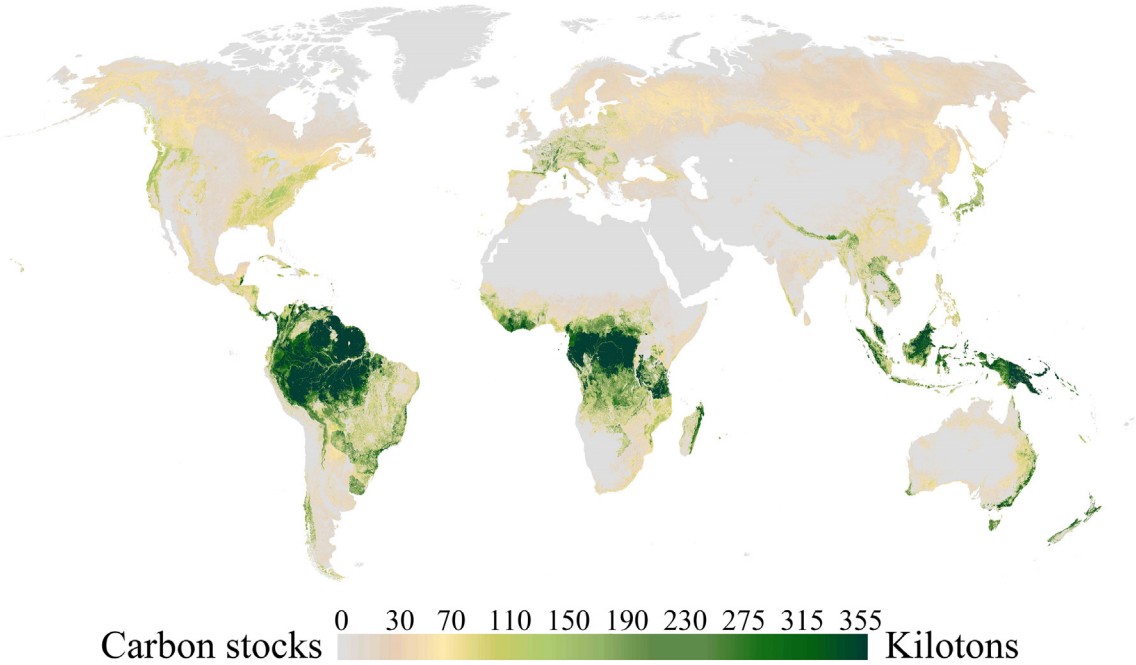

Fig. 1. Gridded global forest carbon stocks (PgC) in 2015 at a spatial resolution of 0.05° × 0.05° latitude/longitude.

factors of BaP subject to biomass burning reported in the literature. As seen, the emission factors reported in these studies vary considerably. This is expected because PAH emissions largely depend on the type of wood, fuel moisture, and experimental conditions.

Based on the emission factors shown in Table 2, we averaged these literature reported emission factors to obtain a mean emission factor of 0.5 mg/kg dry matter for BaP. Considering that our biomass map is shown in unit carbon stocks (tons), the amount of carbon is not in dry matter weight. Given that the carbon stocks in vegetation are very close to 50% (Iinuma et al., 2007; Jenkins et al., 1996), the emission factor can be determined by doubling the dry matters, which often has been used to compile traditional PAH emission inventories (Shen et al., 2013).

Another critical factor in estimates of PAH emissions from biomass burning is combustion efficiency (CE). There are high uncertainties in the calculation of the CE, including high values in the dry season (50–80%) and low values in the rainy season (5–30%). Different types of burning materials always result in different CE values. In tropical and temperate forests, the CE is generally below 30%, and the CE over grasslands and savannas could reach 60%–90% in the drought season and drop below 25% in the rainy season (Seiler and Crutzen, 1980) at values higher than those in forests. In addition to the vegetation type, the CE may also vary in different vegetative organs due to their different structures and moisture content. Leaves have the highest CE, ranging from 80% to 100%; followed by stems, which have a CE below 40%; and the CE for roots is not taken into consideration in forest fires. While surface roots can contribute to the fuel load under high fire severity conditions, their contribution is so small that it can be ignored in CE estimates. The northern boreal forest is a dense forest and is among the least complex and shortest forests in the world. The annual mean temperature in the northern boreal forest region ranges from −12 to 6 °C, and the region only has temperatures higher than 10 °C during three months out of the year (Pan et al., 2013). Taking all these factors into consideration, we chose 20% as a typical CE value for the northern boreal forest. This CE is a reasonable constant that will not lead to false results in PAH emission estimates.

2.3. MODIS burned area

We used the MODIS burned area (hectare) dataset MCD64CMQ Collection 6 to determine the biomass burning areas in the northern boreal forest region and in other vegetation-covered areas. The MCD64 dataset is generated using surface reflectance and active fire input data. In a version of MCD64 released in 2010, the burned area is more sensitive to small and moderate burns, which reduces the burn-data uncertainties (Giglio et al., 2009). MCD64CMQ is a special MODIS burned area dataset that was designated for climate studies. With a moderate grid size (0.25° × 0.25° lat/lon) and a long-term, monthly monitoring period from November 2001 to December 2017, the MCD64CMQ dataset provides both burned area data and the fraction burned over seventeen land cover types that were archived in the MCD12Q1 land cover type data. More information about the MODIS burned area data can be found on the MODIS website (http://modis-fire.umd.edu/, last accessed on July 28, 2019).

2.4. PAH emission estimation

PAH emissions from northern boreal forest fires can be estimated using a simple statistical relationship,

$$EMI = FL \times BA \times EF \times CE, \quad (1)$$

where EMI (ton) is the amount of PAHs emitted from a burned forest; FL (ton/hectare) is the fuel load; BA (hectare) is the burned area, namely, the burned forest; EF (mg/kg) is an emission factor, defined here as the amount of PAHs emitted from one-unit fuel load; and CE (%) is the combustion efficiency. In the present study, the fuel load FL is identical to the carbon stocks. It is worthwhile to note that we did not take the PAH emissions from the burning forest sediment into consideration, which could extend PAH emissions after a forest fire incident (Gabos et al., 2001), due to the lack of monitoring data and reliable methods to quantify soil emission sources.

2.5. Uncertainty analysis

The reconstructed emission inventories from biomass burning are subject to uncertainties. These uncertainties might come from emission factors, the MODIS burned area, carbon stocks, and combustion efficiency. We employed the Monte Carlo model to evaluate uncertainties in the reconstructed emission inventories following the literature-reported methods (Goslee et al., 2014; Holdaway et al., 2014; Metsaranta et al., 2014; Huang et al., 2015). The detailed uncertainty analysis is presented in Supplementary text and Fig. S3.

2.6. GEOS-Chem simulation

Detailed GEOS-Chem model descriptions are presented in Supplementary. Two GEOS-Chem model scenarios were set up to identify the origins of the high Arctic BaP. In the first scenario (S1, also referred to as the “FIRE” simulation), the updated BaP emission inventory from the biomass burning used in this study was input into the GEOS-Chem model to quantify the changes in BaP induced by northern forest biomass burning. In the second model scenario (S2), the PKU-FUEL BaP emission inventory from all emission sectors (http://inventory.pku.edu.cn/,last accessed on July 25, 2019), referred to as the TOTAL simulation, was input into the GEOS-Chem model to repeat the model simulation under the same meteorological fields. The modeling results were verified by measured BaP air concentrations at three Arctic monitoring sites: the Zeppelin Mountain air-monitoring station (Svalbard/Norway, 78° 55′N, 11°56′E, 1992–2014), Alert (Canada, 82°30′N, 62° 19′ W, 1993–2014), and Pallas (Matorova, Finland; 68° 00′ N, 24° 15′ E; 1996–2012). The detailed sampling methods and strategy at these three sites can be found in Hung et al. (2005), and the model evaluation results against measurement data are presented in Supplementary text, Fig. S4, and Table S1.

2.7. Tagging method

A tagging method that was previously used to quantify the source-receptor relationships of black carbon, carbon monoxide, and sulfur dioxide (Rasch et al., 2000; Wang et al., 2014) was employed to assess the contributions of PAH emissions from biomass burning in the northern boreal forest to their fluctuation. The tagging method separates the entire emission inventory into different potential source regions and examines their respective contributions to pollutant concentrations using a simple matrix that examines the sensitivity of concentrations from a receptor region to source regions. Here, the Canadian, Russian, and European boreal forest regions, where PAHs were likely emitted due to the occurrence of forest fires, were selected to assess the source-receptor relationships as shown in Fig. S6. The three receptors were set at the three PAH monitoring sites across the Arctic as shown in Fig. S5. The tagging method can be defined as

$$C_{ij} = A_{ij}/A_j, \quad (2)$$

where $C_{i,j}$ is the fractional contribution of the ith PAH emission region to the jth receptor, and $A_{i,j}$ is the PAH concentration in receptor region *j* tracking back to its ith source region, and A_j is the BaP concentration in the jth receptor attributable to all source regions defined by $A_j = \sum_i A_{ij}$.

3. Results and discussion

3.1. Long term trends of boreal forest fires

The northern boreal forest (Fig. S6) occupies an area of 1135.2×10^6 ha and has an estimated carbon stock of over 53.9 PgC, accounting for 13.7% of the world's total forest carbon stocks (Pan et al., 2013). The northern boreal forest plays a key role in land-atmosphere substance transport (Dong et al., 2003; Pan et al., 2013). Recent studies have reported an increasing trend of forest fire frequency in the northern boreal forest region (Gillett et al., 2004; Seidl et al., 2014; Shvidenko et al., 2011; Stocks et al., 1998; Westerling et al., 2006), and forest fires have been identified as the dominant factor in boreal forest loss in the past two decades (Hansen et al., 2013; Potapov et al., 2008). Fig. 2 displays the total annual burned areas from 2001 to 2017 across the three northern boreal forest regions in Canada (Fig. 2b), Europe (Fig. 2c), and Russia (Fig. 2d). The Canadian boreal forest burned area has peaks from 2002 to 2005 and from 2012 to 2015. During the two periods, the annual mean burned area was 4.12×10^6 ha, which is 1.5 times larger than the mean boreal forest burned area averaged over 2002 to 2017. The Canadian boreal forest is the only boreal forest region with an increasing burned area. The European boreal burned area did not exhibit a significant trend from 2002 to 2017, but its trend did fluctuate during this period. The mean burned area in the European boreal forest is estimated to be 2.45×10^5 ha from 2002 to 2017. Given its considerably large size (Fig. 2), the Russian boreal forest is considered the major source of the northern boreal forest burned area, accounting for 81.5% of the total burned area in the northern boreal forest. Fig. S7 shows the monthly burned area averaged over each of the three northern boreal regions. Unlike the burned areas in the Canadian boreal forest, which were unimodal and were at their highest in the summer months of June, July, and August, the burned areas in the European and Russian boreal forest exhibited a bimodal pattern with the highest burned area from July to September and the other peaks in March (European) and April (Russian). These peaks were likely associated with the early snowmelt and dry conditions in the spring in these two regions.

3.2. Influence of northern boreal forest biomass burning on BaP fluctuations

In the subsequent discussions, we report the responses of BaP atmospheric concentrations in the high Arctic to its emissions from different burned areas in the different northern boreal forest regions. Fig. 3 compares the updated BaP emission inventory from the northern boreal forest wildfires with the PKU BaP emission inventory from wildfire and deforestation emission sector in the three northern boreal forest regions (Fig. S6) from 2002 to 2014. The BaP emissions from the two inventories exhibit similar annual fluctuations, but the updated BaP inventory from the northern boreal forest wildfires shows higher emissions in the northern boreal forest region as a whole (Fig. 3a) and in the European

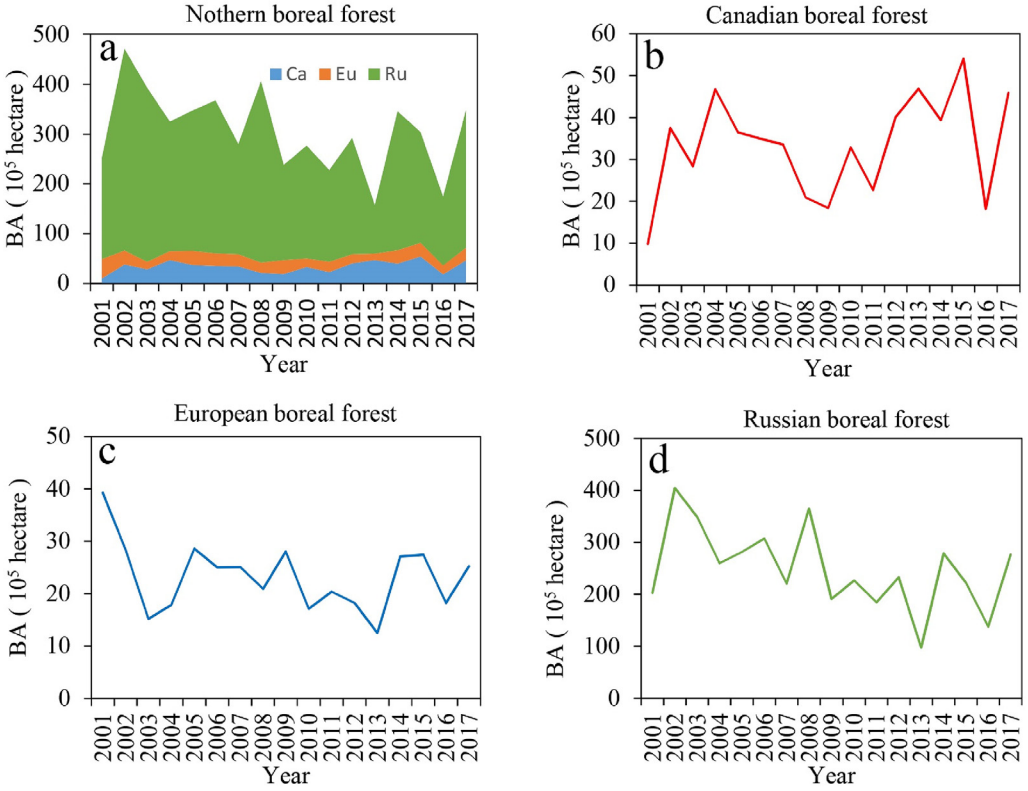

Fig. 2. Annual burned area (BA) in the northern boreal forests in three continents and countries from 2002 to 2017. (a) BA in the three boreal forests, (b) BA in the Canadian boreal forest, (c) BA in the European boreal forest, and (d) BA in the Russian boreal forest.

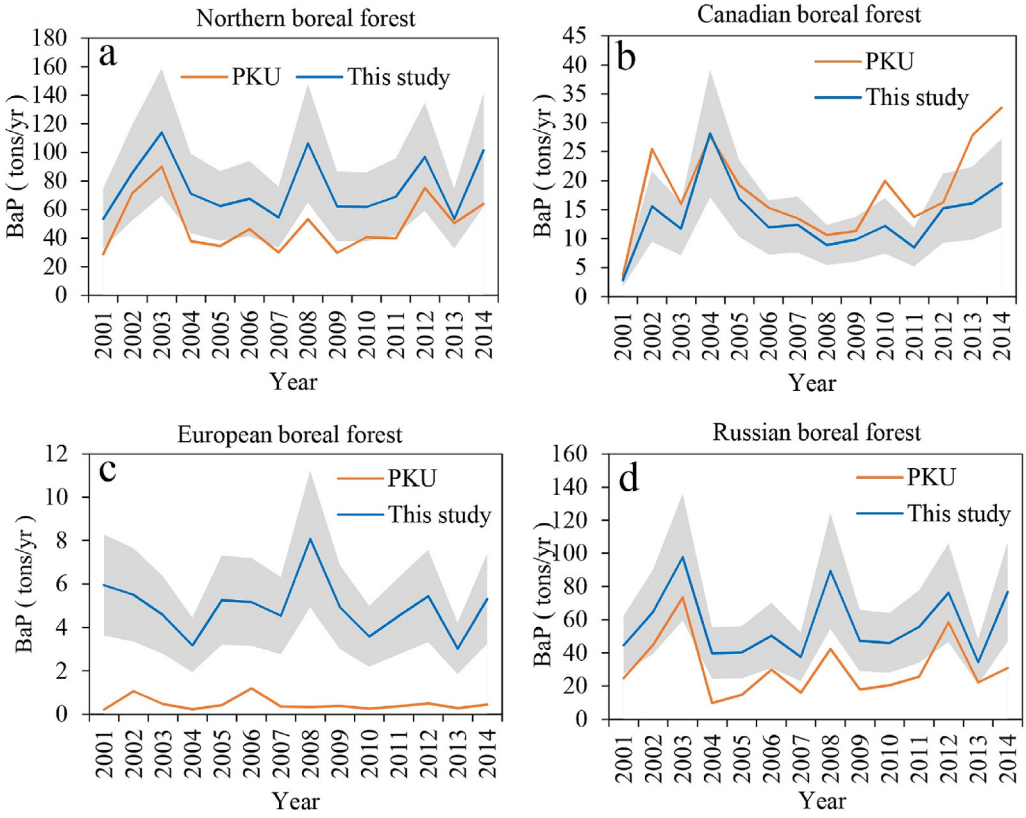

Fig. 3. Updated annual BaP emissions (ton/yr) developed in the present study (blue solid line) and from PKU-FUEL (yellow solid line) wildfire and deforestation emission sector from 2001 to 2014. (a) BaP emissions in the entire northern boreal forest; (b) BaP emissions from the Canadian boreal forest; (c) BaP emissions from the European boreal forest; and (d) BaP emissions from the Russian boreal forest. The gray shading highlights emission uncertainty (1σ) estimated from Monte-Carlo simulation (Supplementary). (For interpretation of the references to colour in this figure legend, the reader is referred to the Web version of this article.)

(Fig. 3c) and Russian (Fig. 3d) boreal forest regions. The updated inventory is, to some extent, in line with the PKU inventory but yields higher BaP emissions in the European and Russian boreal forest regions. The main difference between the two BaP emission inventories from wildfires is that the wildfire and deforestation emission sector in the PKU inventory was constructed based on the Global Fire Emission Database (http://www.globalfiredata.org/, last accessed on July 25, 2019) in which the burned areas were directly collected from MODIS satellite remote sensing data, whereas our updated BaP inventory from wildfires used the surface carbon storage and improved emission factors.

The GEOS-Chem modeled BaP concentrations from the two model scenarios at the three Arctic sites from 2002 to 2014 are displayed in Fig. 4. Fig. S8 shows the GEOS-Chem simulated global BaP concentrations from the FIRE model scenario (Fig. S8a) and the TOTAL model scenario (Fig. S8b). By comparing the modeling results from the two scenarios, it can be seen from Fig. 4 that, as expected, the modeled BaP air concentrations (solid purple line) from the FIRE simulation using the updated biomass burning induced BaP emissions are lower than the monitored data at the three Arctic sites. However, at the two higher Arctic sites Alert (82°30′N, Fig. 4a) and Zeppelin (76°55′ N, Fig. 4b), the BaP emissions from northern boreal forest wildfires yielded higher BaP air concentrations than those from the Pallas site, which is located in a relatively lower latitude of the Arctic (68° 00′ N, Fig. 4c). The modeled BaP concentrations from the TOTAL scenario simulation are slightly higher than the measured concentrations at the three sites, but the changes in the annual BaP concentrations simulated from this scenario agreed reasonably well with the measured BaP concentrations at the three sampling sites, as shown in Fig. 4, particularly at the Zeppelin and Pallas sites. GEOS-Chem modeled BaP concentrations were usually lower than the measured value at the Alert site before 2006. After 2006, the modeled concentrations matched better with sampled data as compared with PKU inventory, though they were higher than the in-situ measurement after 2012, as shown in Fig. 4a. Overall, the updated emission inventory improved BaP prediction at the Alert site, as shown in Fig. 3. The updated inventory significantly enhanced BaP emissions in European and Russian boreal forest regions but decreased BaP emission levels in the Canadian boreal forest region, particularly after 2010. Fig. 4 shows that the modeled BaP concentrations from the FIRE scenario simulation were lower than those from the TOTAL scenario simulation, but the updated BaP emissions from wildfires were lower than the PKU inventory from all emission sectors. It should be noted that Fig. 3 compares the updated BaP emission inventory from wildfires (i.e., FIRE inventory) and PKU BaP emission inventory from wildfire only. The latter only accounts for 17% of BaP emission from all six emission sectors in PKU BaP inventory (Shen et al., 2013). Fig. 5 displays the percent contribution of northern boreal forest fires to BaP air concentrations at the three Arctic sites, calculated by the GEOS-Chem modeled BaP concentration ratios of the FIRE run (scenario 1) to the TOTAL run (scenario 2) from 2002 to 2014. The results further revealed strong contributions of northern boreal forest wildfires to BaP formation and temporal variations at the Alert and Zeppelin sites, accounting for 28.7% of the mean BaP levels at Alert (solid red line) and 17.9% at Zeppelin (solid purple line), averaged over the period from 2002 to 2014. In some cases, e.g., in September 2004 and October 2013, our

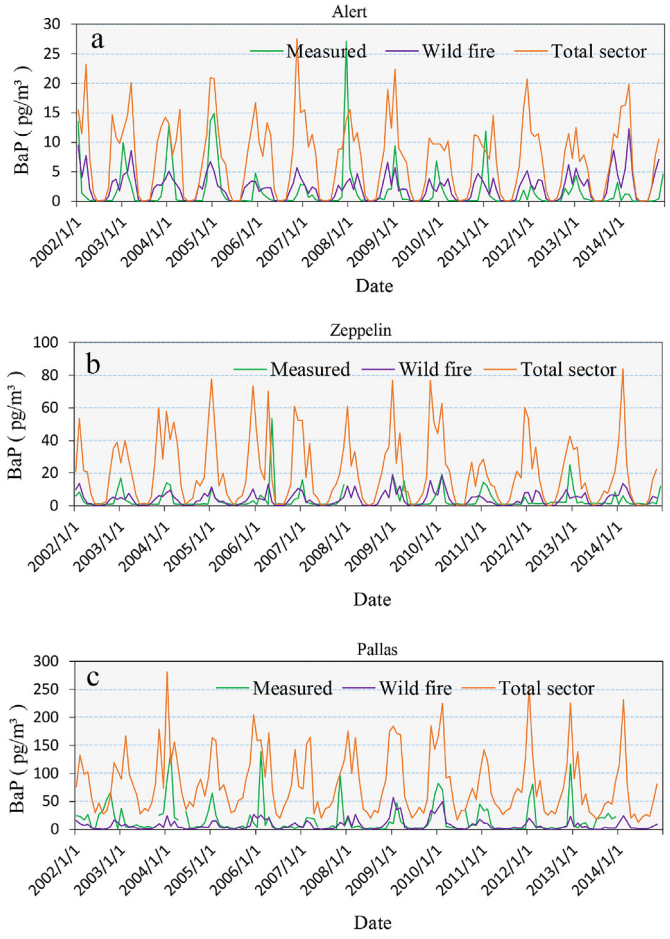

Fig. 4. GEOS-Chem simulated BaP air concentrations (pg/m^3) from the FIRE and TOTAL model scenarios and sampled BaP concentrations at the Alert (a), Zeppelin (b), and Pallas (c) sampling sites.

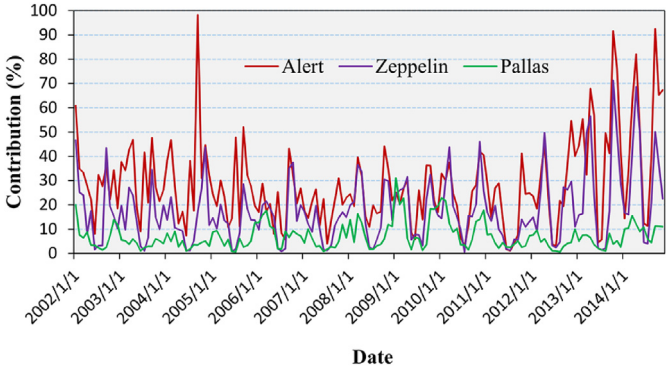

Fig. 5. Percent contributions (%) of northern boreal forest fire-induced BaP air concentrations at the three Arctic sites calculated by the GEOS-Chem modeled BaP concentration ratios of the FIRE run (scenario 1) to the TOTAL run (scenario 2), namely, FIRE/TOTAL, from 2002 to 2014.

modeled result show that northern boreal forest biomass burning contributed over 90% to the modeled BaP at the Alert site. Conversely, at the lower Arctic site of Pallas, wildfires contributed merely 7% to the mean BaP concentration averaged over the same period (solid green line). It is worth noting that both the BaP emissions and the burned area in the Canadian boreal forest region inclined from 2012 onward (Figs. 2 and 3). Our modeled percentage contribution of forest fire-induced BaP concentrations averaged over the period from 2012 to 2014 increased 41% at Alert, 26% at Zeppelin, and 10% at Pallas. However, no significant increasing trends of BaP emissions were observed in the European and Russian boreal forest regions. These results indicate that the effect of northern boreal forest biomass burning on BaP concentrations was enhanced toward higher latitudes in the Arctic. In the lower Arctic, such as Pallas, there are more substantial human residential and tourist activities, which form large PAH emission sources that might overwhelm natural PAH emissions (Yu et al., 2019). The Zeppelin site also experiences moderate human activities, particularly during the summertime (Hung et al., 2005). At the high Arctic site Alert, there are almost no human activities throughout the year. In this case, wildfires play a more important role in changes in BaP levels. Moreover, increasing BaP emissions (Fig. 3) from the northern boreal forest burned area (Fig. 2b and d) could contribute more to BaP contamination in the Arctic environment. Therefore, if the Arctic warming trend continues in the future, locally emitted PAHs, including BaP induced by Arctic forest biomass burning, would likely persist and increase.

It should also be noted that the modeled BaP concentrations at the three Arctic monitoring sites from the FIRE simulation (Fig. 4) seem to correspond well to the temporal variations of the burned area (Fig. 2) and the BaP emissions in the three northern boreal forest regions (Fig. 3). This is particularly evident at the Alert site, where the modeled BaP concentrations agree with the burned area and emissions from the Canadian boreal forest region.

3.3. *Tagging BaP sources from northern boreal forest biomass burning*

The responses of BaP concentrations at the three the Arctic monitoring sites to forest fires from different northern boreal forest regions were assessed numerically by the tagging method (section 2.7). The results are illustrated in Fig. 6**.** The forest fires from the Canadian boreal forest region made the largest contribution of 69.4% to the BaP concentration at the high Arctic Alert site averaged over the period from 2003 to 2014 (excluding 2002 as the spin-up period), followed by the wildfires from the Russian boreal forest at 21.1%. At the two European monitoring sites, our modeling results using the tagging technique indicate that forest biomass burning from the Russian boreal forest region contributed 78.9% and 70.1% of the BaP levels at the Zeppelin and Pallas sites, respectively, followed by the European boreal forest region. However, the wildfires from the Canadian boreal forest made an almost identical contribution to the BaP concentration at the Zeppelin site compared to the fires in the European boreal forest. Fig. S9 shows the accumulated MODIS-monitored active fire mean power from 2000 to 2016

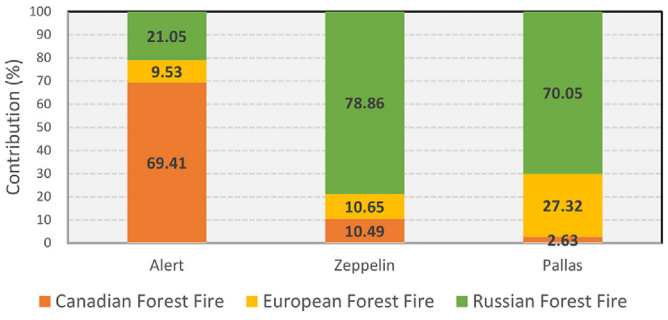

Fig. 6. Percent contribution (%) of the boreal forests in Canada, Europe, and Russia to the mean BaP air concentrations averaged over the period from 2003 to 2014 at the three Arctic sampling sites.

superimposed by the mean vector winds in the warm season (May to September) averaged over the period 2002 to 2016 from 40 to 90°N across the Northern Hemisphere. A considerably larger number of fire points can be observed in the boreal forest regions extending from the Northwest Territories to northern Quebec of Canada and Northern Russia, particularly in the region of Siberia; these regions are compared with the fire points in the European boreal forest region. The smaller number of fire points in the European boreal forest could be partly attributed to its smaller area compared to Canada and Russia. The mean wind vectors during the warm season show westerly and southwesterly wind components in the Canadian sub-Arctic and Arctic regions and northerly and northeasterly wind components in the Russian Arctic region. Because Alert is located at an inland high Arctic site and forest fires occur far away from oceans, wildfires induced BaP emission and concentration caused by relatively arid environments release PAHs are then delivered by favorable westerly and southwesterly wind flows to the high Arctic. Conversely, the European northern boreal forest region is proximate to the north Atlantic Ocean and the North Sea, where westerly (onshore) winds often prevail (Fig. S9), conveying relatively cold and humid air in the warm season into the European continent and boreal forest region and thus reducing the frequency of forest fires.

4. Conclusions

The increasing trend of some PAH congeners in the high Arctic since the 2000s provides evidence for increasing forest fire contributions to the emission of toxic chemicals in the Arctic. To quantitatively assess the contribution of Arctic forest fires to the environmental fate of PAHs, we first developed a new PAH emission inventory from forest biomass burning using both the MODIS burned area and carbon stock data. We showed that this new inventory improved the underestimation of PAH air emissions associated with biomass burning in the high Arctic. By implementing the new BaP emissions into the GEOS-Chem atmospheric chemistry model, we simulated the contributions of increasing wildfires from the northern boreal forest region to BaP environmental contamination. The modeling results from the two scenario model runs revealed that the boreal forest area, atmospheric circulation/wind patterns, and different site locations all contributed to the BaP concentrations at the different Arctic sampling sites, located in the high Canadian Arctic and the European Arctic. It was found that increasing wildfires from the northern boreal forest associated with the Arctic warming enhanced BaP emissions and led to increased BaP levels in the Canadian and European Arctic. This was particularly evident from 2012 onward, when the increasing amount of burned area due to boreal forest fires promoted significantly increased BaP emissions and concentration levels across the Arctic. We showed that the northern boreal forest fires in Russia made a major contribution to BaP fluctuations at European Arctic sampling sites, and the change in biomass burning induced BaP concentrations at Canadian high Arctic site, Alert, was primarily attributed to Canada's northern boreal forest wildfires. Our results revealed that rapid Arctic warming would likely further enhance PAH contamination to the Arctic environment by increasing the frequency of wildfires in the northern boreal forests. This could offset the decline in air pollutants in the Arctic resulting from worldwide efforts to reduce air emissions.

Declaration of competing interest

The authors declare no competing financial interest.

CRediT authorship contribution statement

Jinmu Luo: Writing - original draft, Methodology, Formal analysis. **Yunman Han:** Formal analysis. **Yuan Zhao:** Formal analysis, Visualization. **Yufei Huang:** Formal analysis, Investigation. **Xinrui Liu:** Investigation, Data curation. **Shu Tao:** Data curation, Writing - review & editing. **Junfeng Liu:** Writing - review & editing. **Tao Huang:** Investigation, Methodology. **Linfei Wang:** Formal analysis. **Kaijie Chen:** Formal analysis. **Jianmin Ma:** Conceptualization, Formal analysis, Writing - original draft, Funding acquisition.

Acknowledgements

This work is supported by National Key R&D Program of China (2017YFC0212002), and the National Natural Science Foundation of China (U1806207). We also acknowledge useful discussions with Dr. N.E. Selin and Dr. Yantosca- Robert M in the course of setting up GEOS-Chem for PAH simulations.

Appendix A. Supplementary data

Supplementary data to this article can be found online at https://doi.org/10.1016/j.envpol.2020.114186.

References

Baccini, A., Goetz, S.J., Walker, W.S., Laporte, N.T., Sun, M., Sulla-Menashe, D., Hackler, J., Beck, P.S.A., Dubayah, R., Friedl, M.A., Samanta, S., Houghton, R.A., 2012. Estimated carbon dioxide emissions from tropical deforestation improved by carbon-density maps. Nat. Clim. Change 2, 182–185. https://doi.org/10.1038/nclimate1354.

Bar-On, Y.M., Phillips, R., Milo, R., 2018. The biomass distribution on Earth. Proc. Natl. Acad. Sci. Unit. States Am. 115, 6506–6511. https://doi.org/10.1073/pnas.1711842115.

Dong, J., Kaufmann, R.K., Myneni, R.B., Tucker, C.J., Kauppi, P.E., Liski, J., Buermann, W., Alexeyev, V., Hughes, M.K., 2003. Remote sensing estimates of boreal and temperate forest woody biomass: carbon pools, sources, and sinks. Remote Sens. Environ. 84, 393–410. https://doi.org/10.1016/S0034-4257(02)00130-X.

Erb, K.-H., Fetzel, T., Plutzar, C., Kastner, T., Lauk, C., Mayer, A., Niedertscheider, M., Körner, C., Haberl, H., 2016. Biomass turnover time in terrestrial ecosystems halved by land use. Nat. Geosci. 9, 674–678. https://doi.org/10.1038/ngeo2782.

Erb, K.-H., Kastner, T., Plutzar, C., Bais, A.L.S., Carvalhais, N., Fetzel, T., Gingrich, S., Haberl, H., Lauk, C., Niedertscheider, M., Pongratz, J., Thurner, M., Luyssaert, S., 2018. Unexpectedly large impact of forest management and grazing on global vegetation biomass. Nature 553, 73–76. https://doi.org/10.1038/nature25138.

Fang, J., Brown, S., Tang, Y., Nabuurs, G.-J., Wang, X., Shen, H., 2006. Overestimated biomass carbon pools of the northern mid- and high latitude forests. Clim. Change 74, 355–368. https://doi.org/10.1007/s10584-005-9028-8.

Friedman, Carey L., Selin, Noelle E., 2016. PCBs in the Arctic atmosphere: determining important driving forces using a global atmospheric transport model. Atmos. Chem. Phys. 16, 3433–3448.

Friedman, C.L., Selin, N.E., 2012. Long-range atmospheric transport of polycyclic aromatic hydrocarbons: a global 3-D model analysis including evaluation of arctic sources. Environ. Sci. Technol. 46, 9501–9510. https://doi.org/10.1021/es301904d.

Friedman, C.L., Zhang, Y., Selin, N.E., 2014. Climate change and emissions impacts on atmospheric PAH transport to the arctic. Environ. Sci. Technol. 48, 429–437. https://doi.org/10.1021/es403098w.

Gabos, S., Ikonomou, M.G., Schopflocher, D., Fowler, B.R., White, J., Prepas, E., Prince, D., Chen, W., 2001. Characteristics of PAHs, PCDD/Fs and PCBs in sediment following forest fires in northern Alberta. Chemosphere, Dioxin '99 43, 709–719. https://doi.org/10.1016/S0045-6535(00)00424-0.

Galarneau, E., Makar, P.A., Sassi, M., Diamond, M.L., 2007. Estimation of atmospheric emissions of six semivolatile polycyclic aromatic hydrocarbons in southern Canada and the United States by use of an emissions processing system. Environ. Sci. Technol. 41, 4205–4213. https://doi.org/10.1021/es062303k.

Giglio, L., Loboda, T., Roy, D.P., Quayle, B., Justice, C.O., 2009. An active-fire based burned area mapping algorithm for the MODIS sensor. Remote Sens. Environ. 113, 408–420. https://doi.org/10.1016/j.rse.2008.10.006.

Gillett, N.P., Weaver, A.J., Zwiers, F.W., Flannigan, M.D., 2004. Detecting the effect of climate change on Canadian forest fires. Geophys. Res. Lett. 31 https://doi.org/10.1029/2004GL020876.

Goslee, K., Walker, S.M., Grais, A., Murray, L., Casarim, F., Brown, S., 2014. Module C-CS: calculations for estimating carbon stocks. Global Canopy available at: http://

theredddesk.org/node/5672.
Haberl, H., Erb, K.H., Krausmann, F., Gaube, V., Bondeau, A., Plutzar, C., Gingrich, S., Lucht, W., Fischer-Kowalski, M., 2007. Quantifying and mapping the human appropriation of net primary production in earth's terrestrial ecosystems. Proc. Natl. Acad. Sci. Unit. States Am. 104, 12942–12947. https://doi.org/10.1073/pnas.0704243104.
Hansen, M.C., Potapov, P.V., Moore, R., Hancher, M., Turubanova, S.A., Tyukavina, A., Thau, D., Stehman, S.V., Goetz, S.J., Loveland, T.R., Kommareddy, A., Egorov, A., Chini, L., Justice, C.O., Townshend, J.R.G., 2013. High-resolution global maps of 21st-century forest cover change. Science 342, 850–853. https://doi.org/10.1126/science.1244693.
Holdaway, R.J., McNeil, S.J., Mason, N.W.H., Carswel, F.E., 2014. Propagating uncertainty in plot-based estimates of forest carbon stock and carbon stock change. Ecosystems. https://doi.org/10.1007/s10021-014-9749-5.
Huang, T., Tian, C., Zhang, K., Gao, H., Li, Y.-F., Ma, J., 2015. Gridded atmospheric emission inventory of 2,3,7,8-TCDD in China. Atmos. Environ. Times 108, 41–48. https://doi.org/10.1016/j.atmosenv.2015.02.070.
Hung, H., Blanchard, P., Halsall, C.J., Bidleman, T.F., Stern, G.A., Fellin, P., Muir, D.C.G., Barrie, L.A., Jantunen, L.M., Helm, P.A., Ma, J., Konoplev, A., 2005. Temporal and spatial variabilities of atmospheric polychlorinated biphenyls (PCBs), organochlorine (OC) pesticides and polycyclic aromatic hydrocarbons (PAHs) in the Canadian Arctic: results from a decade of monitoring. Sci. Total Environ. 342, 119–144. https://doi.org/10.1016/j.scitotenv.2004.12.058. Sources, Occurrence, Trends and Pathways of Contaminants in the Arctic.
Hung, H., Katsoyiannis, A.A., Brorström-Lundén, E., Olafsdottir, K., Aas, W., Breivik, K., Bohlin-Nizzetto, P., Sigurdsson, A., Hakola, H., Bossi, R., Skov, H., Sverko, E., Barresi, E., Fellin, P., Wilson, S., 2016. Temporal trends of persistent organic pollutants (POPs) in arctic air: 20 years of monitoring under the arctic monitoring and assessment programme (AMAP). Environ. Pollut. 217, 52–61. https://doi.org/10.1016/j.envpol.2016.01.079. Persistent organic pollutants (POPs): Trends, Sources and Transport Modelling.
Iinuma, Y., Brüggemann, E., Gnauk, T., Müller, K., Andreae, M.O., Helas, G., Parmar, R., Herrmann, H., 2007. Source characterization of biomass burning particles: the combustion of selected European conifers, African hardwood, savanna grass, and German and Indonesian peat. J. Geophys. Res. Atmos. 112 https://doi.org/10.1029/2006JD007120.
Jenkins, B.M., Jones, A.D., Turn, S.Q., Williams, R.B., 1996. Emission factors for polycyclic aromatic hydrocarbons from biomass burning. Environ. Sci. Technol. 30, 2462–2469. https://doi.org/10.1021/es950699m.
Kakareka, S.V., Kukharchyk, T.I., Khomich, V.S., 2005. Study of PAH emission from the solid fuels combustion in residential furnaces. Environ. Pollut. 133, 383–387. https://doi.org/10.1016/j.envpol.2004.01.009.
Kim, J., Kug, J., Jeong, S., Park, H., Schaepman-Strub, G., 2020. Extensive fires in southeastern Siberian permafrost linked to preceding Arctic Oscillation. Sci. Adv. 26 https://doi.org/10.1126/sciadv.aax3308.
Kim Oanh, N.T., Albina, D.O., Ping, L., Wang, X., 2005. Emission of particulate matter and polycyclic aromatic hydrocarbons from select cookstove–fuel systems in Asia. Biomass Bioenergy 28, 579–590. https://doi.org/10.1016/j.biombioe.2005.01.003.
Kim Oanh, N.T., Bætz Reutergårdh, L., Dung, N.T., 1999. Emission of polycyclic aromatic hydrocarbons and particulate matter from domestic combustion of selected fuels. Environ. Sci. Technol. 33, 2703–2709. https://doi.org/10.1021/es980853f.
Kong, D., MacLeod, M., Hung, H., Cousins, I.T., 2014. Statistical analysis of long-term monitoring data for persistent organic pollutants in the atmosphere at 20 monitoring stations broadly indicates declining concentrations. Environ. Sci. Technol. 48, 12492–12499. https://doi.org/10.1021/es502909n.
Laender, F.D., Hammer, J., Hendriks, A.J., Soetaert, K., Janssen, C.R., 2011. Combining monitoring data and modeling identifies PAHs as emerging contaminants in the arctic. Environ. Sci. Technol. 45, 9024–9029. https://doi.org/10.1021/es202423f.
Lee, R.G.M., Coleman, P., Jones, J.L., Jones, K.C., Lohmann, R., 2005. Emission factors and importance of PCDD/Fs, PCBs, PCNs, PAHs and PM10 from the domestic burning of coal and wood in the U.K. Environ. Sci. Technol. 39, 1436–1447. https://doi.org/10.1021/es048745i.
Ma, J., Hung, H., Macdonald, R.W., 2016. The influence of global climate change on the environmental fate of persistent organic pollutants: a review with emphasis on the Northern Hemisphere and the Arctic as a receptor. Global Planet. Change 146, 89–108. https://doi.org/10.1016/j.gloplacha.2016.09.011.
Ma, J., Hung, H., Tian, C., Kallenborn, R., 2011. Revolatilization of persistent organic pollutants in the Arctic induced by climate change. Nat. Clim. Change 1, 255–260. https://doi.org/10.1038/nclimate1167.
MacDicken, K.G., 2015. Global forest resources assessment 2015: what, why and how? For. Ecol. Manag. 352 https://doi.org/10.1016/j.foreco.2015.02.006, 3–8.
Malevsky-Malevich, S.P., Molkentin, E.K., Nadyozhina, E.D., Shklyarevich, O.B., 2008. An assessment of potential change in wildfire activity in the Russian boreal forest zone induced by climate warming during the twenty-first century. Climatic Change 86, 463–474. https://doi.org/10.1007/s10584-007-9295-7.
Metsaranta, J.M., Shaw, C.H., Kurz, W.A., Boisvenue, C., Morken, S., 2014. Uncertainty of Inventory-Based Estimates of the Carbon Dynamics of Canada's Managed Forest (1990–2014). NRC press available at: https://www.nrcresearchpress.com/doi/full/10.1139/cjfr-2017-0088#.Xab2Mn-9MnU.
Miura, K., Shimada, K., Sugiyama, T., Sato, K., Takami, A., Chan, C.K., Kim, I.S., Kim, Y.P., Lin, N.-H., Hatakeyama, S., 2019. Seasonal and annual changes in PAH concentrations in a remote site in the Pacific Ocean. Sci. Rep. (Nat. Publ. Group); Lond. 9, 1–10. https://doi.org/10.1038/s41598-019-47409-.
Muntean, M., Janssens-Maenhout, G., Guizzardi, D., Crippa, M., Schaaf, E., Olivier, J.G., Dentener, F.J., 2016. EDGARv4 Gridded Anthropogenic Emissions of Persistent Organic Pollutants (POPs) from Power Generation, Residential and Transport Sectors: Regional Trends Analysis in East Asia. American Geophysical Union, Fall Meeting, 2016, abstract #A12B-05.
Pan, Y., Birdsey, R.A., Fang, J., Houghton, R., Kauppi, P.E., Kurz, W.A., Phillips, O.L., Shvidenko, A., Lewis, S.L., Canadell, J.G., Ciais, P., Jackson, R.B., Pacala, S.W., McGuire, A.D., Piao, S., Rautiainen, A., Sitch, S., Hayes, D., 2011. A large and persistent carbon sink in the world's forests. Science 333, 988–993. https://doi.org/10.1126/science.1201609.
Pan, Y., Birdsey, R.A., Phillips, O.L., Jackson, R.B., 2013. The structure, distribution, and biomass of the world's forests. Annu. Rev. Ecol. Evol. Syst. 44, 593–622. https://doi.org/10.1146/annurev-ecolsys-110512-135914.
Potapov, P., Hansen, M.C., Stehman, S.V., Loveland, T.R., Pittman, K., 2008. Combining MODIS and Landsat imagery to estimate and map boreal forest cover loss. Remote Sens. Environ. 112, 3708–3719. https://doi.org/10.1016/j.rse.2008.05.006.
Rasch, P.J., Barth, M.C., Kiehl, J.T., Schwartz, S.E., Benkovitz, C.M., 2000. A description of the global sulfur cycle and its controlling processes in the national center for atmospheric research community climate model, version 3. J. Geophys. Res. Atmos. 105, 1367–1385. https://doi.org/10.1029/1999JD900777.
Ravindra, K., Sokhi, R., Van Grieken, R., 2008. Atmospheric polycyclic aromatic hydrocarbons: source attribution, emission factors and regulation. Atmos. Environ. 42, 2895–2921. https://doi.org/10.1016/j.atmosenv.2007.12.010.
Saatchi, S.S., Harris, N.L., Brown, S., Lefsky, M., Mitchard, E.T.A., Salas, W., Zutta, B.R., Buermann, W., Lewis, S.L., Hagen, S., Petrova, S., White, L., Silman, M., Morel, A., 2011. Benchmark map of forest carbon stocks in tropical regions across three continents. Proc. Natl. Acad. Sci. Unit. States Am. 108, 9899–9904. https://doi.org/10.1073/pnas.1019576108.
Schauer, J.J., Kleeman, M.J., Cass, G.R., Simoneit, B.R.T., 2001. Measurement of emissions from air pollution sources. 3. C1–C29 organic compounds from fireplace combustion of wood. Environ. Sci. Technol. 35, 1716–1728. https://doi.org/10.1021/es001331e.
Schifman, L.A., Boving, T.B., 2015. Spatial and seasonal atmospheric PAH deposition patterns and sources in Rhode Island. Atmos. Environ. 120, 253–261. https://doi.org/10.1016/j.atmosenv.2015.08.056.
Seidl, R., Schelhaas, M.-J., Rammer, W., Verkerk, P.J., 2014. Increasing forest disturbances in Europe and their impact on carbon storage. Nat. Clim. Change 4, 806–810. https://doi.org/10.1038/nclimate2318.
Seiler, W., Crutzen, P.J., 1980. Estimates of gross and net fluxes of carbon between the biosphere and the atmosphere from biomass burning. Climatic Change 2, 207–247. https://doi.org/10.1007/BF00137988.
Shen, H., Huang, Y., Wang, R., Zhu, D., Li, W., Shen, G., Wang, B., Zhang, Y., Chen, Y., Lu, Y., Chen, H., Li, T., Sun, K., Li, B., Liu, W., Liu, J., Tao, S., 2013. Global atmospheric emissions of polycyclic aromatic hydrocarbons from 1960 to 2008 and future predictions. Environ. Sci. Technol. 47, 6415–6424. https://doi.org/10.1021/es400857z.
Shvidenko, A.Z., Shchepashchenko, D.G., Vaganov, E.A., Sukhinin, A.I., Maksyutov, Sh.Sh., McCallum, I., Lakyda, I.P., 2011. Impact of wildfire in Russia between 1998–2010 on ecosystems and the global carbon budget. Dokl. Earth Sci. 441, 1678–1682. https://doi.org/10.1134/S1028334X11120075.
Simard, M., Pinto, N., Fisher, J.B., Baccini, A., 2011. Mapping forest canopy height globally with spaceborne lidar. J. Geophys. Res. Biogeosci. 116 https://doi.org/10.1029/2011JG001708.
Stocks, B.J., Fosberg, M.A., Lynham, T.J., Mearns, L., Wotton, B.M., Yang, Q., Jin, J.-Z., Lawrence, K., Hartley, G.R., Mason, J.A., Mckenney, D.W., 1998. Climate change and forest fire potential in Russian and Canadian boreal forests. Climatic Change 38, 1–13. https://doi.org/10.1023/A:1005306001055.
Stohl, A., Berg, T., Burkhart, J.F., Fjæraa, A.M., Forster, C., Herber, A., Hov, Ø., Lunder, C., McMillan, W.W., Oltmans, S., Shiobara, M., Simpson, D., Solberg, S., Stebel, K., Ström, J., Tørseth, K., Treffeisen, R., Virkkunen, K., Yttri, K.E., 2007. Arctic smoke – record high air pollution levels in the European Arctic due to agricultural fires in Eastern Europe in spring 2006. Atmos. Chem. Phys. 7, 511–534. https://doi.org/10.5194/acp-7-511-2007.
Thurner, M., Beer, C., Santoro, M., Carvalhais, N., Wutzler, T., Schepaschenko, D., Shvidenko, A., Kompter, E., Ahrens, B., Levick, S.R., Schmullius, C., 2014. Carbon stock and density of northern boreal and temperate forests. Global Ecol. Biogeogr. 23, 297–310. https://doi.org/10.1111/geb.12125.
Treffeisen, R., Tunved, P., Ström, J., Herber, A., Bareiss, J., Helbig, A., Stone, R.S., Hoyningen-Huene, W., Krejci, R., Stohl, A., Neuber, R., 2007. Arctic smoke – aerosol characteristics during a record smoke event in the European Arctic and its radiative impact. Atmos. Chem. Phys. 7, 3035–3053. https://doi.org/10.5194/acp-7-3035-2007.
Vakkari, V., Beukes, J.P., Maso, M.D., Aurela, M., Josipovic, M., Zyl, P.G. van, 2018. Major secondary aerosol formation in southern African open biomass burning plumes. Nat. Geosci. 11, 580. https://doi.org/10.1038/s41561-018-0170-0.
World Meteorological Organization WMO, 2019. https://public.wmo.int/en/media/news/july-matched-and-maybe-broke-record-hottest-month-analysis-began. (Accessed 25 August 2019).
Wang, H., Rasch, P.J., Easter, R.C., Singh, B., Zhang, R., Ma, P.-L., Qian, Y., Ghan, S.J., Beagley, N., 2014. Using an explicit emission tagging method in global modeling of source-receptor relationships for black carbon in the Arctic: variations, sources, and transport pathways. J. Geophys. Res. Atmos. 119, 12,888–12,909. https://doi.org/10.1002/2014JD022297.
Westerling, A.L., Hidalgo, H.G., Cayan, D.R., Swetnam, T.W., 2006. Warming and

earlier spring increase western U.S. Forest wildfire activity. Science 313, 940–943. https://doi.org/10.1126/science.1128834.
Wilcke, W., 2007. Global patterns of polycyclic aromatic hydrocarbons (PAHs) in soil. Geoderma 141, 157–166. https://doi.org/10.1016/j.geoderma.2007.07.007.
Yu, Y., Katsoyiannis, A., Bohlin-Nizzetto, P., Brorström-Lundén, E., Ma, J., Zhao, Y., Wu, Z., Tych, W., Mindham, D., Sverko, E., Barresi, E., Dryfhout-Clark, H., Fellin, P., Hung, H., 2019. Polycyclic aromatic hydrocarbons not declining in arctic air despite global emission reduction. Environ. Sci. Technol. 53, 2375–2382. https://doi.org/10.1021/acs.est.8b05353.
Zhang, X., Kondragunta, S., 2006. Estimating forest biomass in the USA using generalized allometric models and MODIS land products. Geophys. Res. Lett. 33 https://doi.org/10.1029/2006GL025879.
Zhang, Y., Tao, S., 2009. Global atmospheric emission inventory of polycyclic aromatic hydrocarbons (PAHs) for 2004. Atmos. Environ. 43, 812–819. https://doi.org/10.1016/j.atmosenv.2008.10.050.
Zhao, Y., Wang, L., Luo, J., Huang, T., Tao, S., Liu, J., Yu, Y., Huang, Y., Liu, X., Ma, J., 2019. A deep learning prediction of polycyclic aromatic hydrocarbons in the high arctic. Environ. Sci. Technol. 53, 13238–13245.
http://www.fao.org/forest-resources-assessment/current-assessment/en/, 2015–. (Accessed 25 July 2019).
http://www.fao.org/forest-resources-assessment/current-assessment/en/, 2010–. (Accessed 25 July 2019).